NEUROSCIENCE RESEARCH NOTES

ISSN: 2576-828X

OPEN ACCESS | RESEARCH NOTES

Neural substrates of perception and imagery revealed by fMRI: a pilot study

Yiyun Gong ¹, Aini Ismafairus Abd Hamid ^{1,2*} and Hafidah Umar ^{1,2*}

- ¹ Department of Neurosciences, School of Medical Sciences, Universiti Sains Malaysia, Kelantan, Malaysia.
- ² Brain and Behaviour Cluster, School of Medical Sciences, Universiti Sains Malaysia, Kelantan, Malaysia.
- * Correspondences: aini ismafairus@usm.my, hafidah umar@usm.my; Tel.: +609-7676348

Received: 27 August 2024; Accepted: 4 May 2025; Published: 16 September 2025 Edited by: Indranath Chatterjee (Manchester Metropolitan University, United Kingdom)

Reviewed by: Elza Othman (Universiti Sultan Zainal Abidin, Malaysia); Mazlyfarina Mohamad (Universiti Kebangsaan Malaysia, Malaysia)

https://doi.org/10.31117/neuroscirn.v8i3.392

Abstract: Visual mental imagery, the subjective experience of "seeing" in the absence of sensory input, has long been studied in relation to perception. While considerable evidence points to shared neural mechanisms, the precise nature of their overlap and divergence remains an area of active investigation. The present fMRI study examined brain activation patterns and functional roles of distinct regions during the perception and imagery of animals, utilising a sparse temporal sampling paradigm to control for auditory interference. Seven participants (2 males, 5 females; mean age = 22.57, SD = 0.48) participated in the study. Perception and imagery tasks were conducted separately within a single session to minimise fatigue and motion artefacts. BOLD signals were preprocessed and analysed using SPM12, employing paired t-tests and repeated measures ANOVA. The analysis utilised an uncorrected threshold of p < 0.001 at the voxel level, combined with cluster-level familywise error (FWE) correction at p < 0.05. Results revealed substantial overlap in neural substrates, with perception uniquely engaged in the right medial superior frontal gyrus, suggesting heightened top-down attentional control. In contrast, imagery preferentially activated the left supplementary motor area and right opercular inferior frontal gyrus, implying a greater demand for internal representation and cognitive control. The imagery phase further demonstrated widespread activation across the frontoparietal network and temporal lobe, with image generation eliciting the strongest engagement of auditory and attentional regions. Self-reported vividness during imagery correlated positively with pre-scan vividness scores (p < 0.05), validating the ecological relevance of the task. These findings suggest that while perception and imagery share a common neural foundation, they diverge in the specific cognitive processes they recruit, with imagery placing greater emphasis on internal generation and manipulation of mental representations. The study highlights the dynamic interplay of brain regions supporting visual imagery and its multifaceted nature, offering potential implications for interventions targeting cognitive enhancement and addressing deficits in perception or imagery.

Keywords: Perception; Mental imagery; Visual imagery; Vividness; fMRI

©2025 by Gong *et al.* for use and distribution according to the Creative Commons Attribution (CC BY-NC 4.0) license (https://creativecommons.org/licenses/by-nc/4.0/), which permits unrestricted non-commercial use, distribution, and reproduction in any medium, provided the original author and source are credited.

1.0 INTRODUCTION

Perception and imagery are fundamental cognitive processes that have long captivated researchers. Perception, the process of interpreting sensory input from the external world (Dijkstra et al., 2019), can be exemplified by observing an apple on a table, where its red colour, round shape, and shiny smooth surface are directly experienced through the senses. Imagery, on the other hand, is the ability to create internal representations of sensory experiences without external stimuli (Ganis, 2013; Kosslyn, 2005), for instance, imagining the same apple in your mind, visualising its features even when it is no longer physically present. Both cognitive processes are essential for understanding human cognition.

While neuroimaging studies have revealed substantial overlap in brain activation patterns during perception and imagery tasks, indicating shared neural substrates (Dijkstra et al., 2019; Xie et al., 2020), there is also evidence of distinct neural mechanisms underlying each process (Winlove et al., 2018). One possible explanation is that perception relies more heavily on bottom-up processing that is driven by external sensory input. In contrast, imagery depends largely on top-down processes that regenerate sensory experiences from memory and mental representations.

Functional magnetic resonance imaging (fMRI) studies have been instrumental in identifying both shared and distinct neural activations during perception and imagery across various sensory modalities, including vision (Albers et al., 2013; Breedlove et al., 2020; Dijkstra et al., 2017a; Fulford et al., 2017; Ganis et al., 2004; Johnson & Johnson, 2014; Naselaris et al., 2015; Slotnick et al., 2005), auditory (Amedi et al., 2005), and (Morozova et al., 2024). touch However, neuropsychological case studies have reported instances of patients with impaired perception but intact imagery, and vice versa, suggesting that these processes are not entirely interchangeable (Bartolomeo et al., 1998, 2013; De Gelder et al., 2014; Moro et al., 2007; Thorudottir et al., 2020).

Furthermore, some fMRI studies have revealed subtle differences in brain activation patterns between perception and imagery, particularly in higher-order cortical regions (<u>Amedi et al., 2005</u>; <u>Lee et al., 2011</u>; <u>Koenig-Robert & Pearson, 2020</u>).

Empirical investigations have revealed that the processing of visual perceptual input primarily occurs in the occipital and temporal lobes (Perry & Fallah, 2014;

Riesenhuber & Poggio, 1999). The primary visual cortex (V1) is the initial cortical region to receive external visual information, which is processed according to its receptive fields and organised retinotopically into cortical field maps (Mountcastle, 1997). Several scientific studies have proposed that the mental imagery process elicits similar retinotopic mapping in V1 as visual perception (Albers et al., 2013; Breedlove et al., 2020; Slotnick et al., 2005).

Studies using multivariate pattern analysis have decoded blood oxygen level-dependent (BOLD) activity in the early visual cortex during perception (Johnson & Johnson, 2014; Naselaris et al., 2015). This analysis employed a voxel-wise model adapted from visual perception, incorporating the retinotopic location, spatial frequency, and orientation of perceptual stimuli, thereby supporting the shared neural representation of imagery and perception (Johnson & Johnson, 2014; Naselaris et al., 2015). This overlap extends to higher-level visual cortex across the ventral visual pathway (Albers et al., 2013; Boccia et al., 2021; Johnson & Johnson, 2014; Ragni et al., 2021; Winlove et al., 2018), indicating the involvement of a substantial portion of the ventral perceptual stream in mental imagery.

Despite the overlaps, there are also differences in imagery and perception. For instance, Lee and colleagues (2011) identified an inverse gradient in the distribution of object information between perception and imagery within the visual areas during visual processing. Mental imagery overlaps more with perception in high-level visual regions, representing more category-specific information, than in low-level retinotopic regions, which are reported to be associated with vividness in imagery.

In addition, conflicting evidence persists regarding the neural mechanisms underlying perception and imagery. While some studies highlight the involvement of the primary visual cortex (V1) in imagery (<u>Johnson & Johnson, 2014</u>; <u>Naselaris et al., 2015</u>), others, including Spagna and colleagues (<u>2021</u>), argue that the early visual cortex is not activated during imagery tasks in healthy individuals.

Furthermore, the roles of higher-order regions, such as the frontal and parietal lobes, remain underexplored, despite their proposed contributions to cognitive control, memory retrieval, and mental representation tasks (<u>De Borst et al., 2011</u>; <u>Ganis et al., 2004</u>). These discrepancies underscore the need for additional research to elucidate the shared and distinct neural

substrates involved in perception and imagery, as well as their engagement during various imagery tasks. Addressing these gaps is essential for enhancing our understanding of these processes and their implications for clinical and cognitive neuroscience.

The current study aims to further elucidate the neural mechanisms underlying perception and imagery by directly comparing brain activation patterns during these processes using fMRI. We hypothesise that while perception and imagery will share common neural substrates, there will also be distinct patterns of activation reflecting the unique demands of each process. Specifically, we predict that perception will elicit stronger activation in sensory cortices due to the presence of external stimuli, while imagery will engage higher-order regions involved in memory retrieval and mental representation (Dijkstra et al., 2017b; Lee et al., 2011; Sulfaro et al., 2023). Furthermore, we hypothesise that there will be significant differences in brain activations across imagery tasks and a positive correlation between Vividness of Visual Imagery Questionnaire (VVIQ) scores and vividness ratings obtained during scanning.

To achieve these objectives, we employed a novel fMRI paradigm that includes both perception and imagery tasks using naturalistic stimuli (animal images and sounds). This paradigm will enable us to compare brain activation patterns during the perception and imagery phases, allowing us to investigate the specific brain regions involved in various imagery tasks, including image generation, image inspection, and vividness rating.

The findings from this study hold significant implications for both clinical and cognitive neuroscience. Addressing these discrepancies could enhance interventions for individuals experiencing imagery deficits, such as those with aphantasia or memory disorders, and improve neurorehabilitation strategies. Additionally, the insights gained could inform cognitive training programs designed to enhance visualisation, memory, and creative problem-solving skills in healthy individuals.

2.0 MATERIALS AND METHODS

2.1 Participants

Seven healthy right-handed participants (5 females; mean age = 22.57, SD = 0.48) participated in this study. Participants were recruited utilising a convenience sampling method through advertisements disseminated via social media platforms and university noticeboards. The recruitment specifically targeted undergraduate

students enrolled at the Universiti Sains Malaysia Health Campus. Handedness was assessed using the Edinburgh Handedness Inventory. Right-handed individuals were incorporated into the study design to mitigate potential confounding effects associated with handedness on brain morphology and function. All participants had normal or corrected-to-normal vision and normal hearing, as assessed by the WHO (World Health Organisation, 2018).

The participants' histories of neurological psychological disorders were assessed through selfreported data obtained via a comprehensive prescreening questionnaire administered prior to the recruitment process. Participants were screened for normal imagery ability using the VVIQ (Marks, 1995), with a score of 32 or above required for inclusion. The inclusion criteria required that participants demonstrate adequate proficiency in English comprehension.

To minimise variability in the neuroimaging data, individuals exhibiting claustrophobia, mental health disorders, or limitations in imagery ability were systematically excluded from the study. This study protocol was approved by Jawatankuasa Penyelidikan Manusia (JEPeM), Universiti Sains (study Malaysia protocol code: (USM) USM/JEPeM/22080565). All participants provided written informed consent. Participants received monetary compensation for their participation.

2.2 Experimental stimuli

Audio-visual stimuli consisted of 35 animal images (e.g., lions, cats) paired with corresponding vocalisations (e.g., roaring, meowing) to ensure congruency. The stimuli were sourced from a previous study (<u>Umar et al., 2021</u>). A full list of the stimuli used is provided in the **Table 1**. Images were edited using Adobe Photoshop 2020 software to remove background scenes and standardise image size. A mid-level grey background was applied to all images, consistent with previous studies (<u>Dijkstra et al., 2017b</u>; <u>Ganis et al., 2004</u>; <u>Lee et al., 2011</u>).

Images were presented for 5000 ms using E-Prime on an MRI-safe display monitor reflected onto a mirror inside the MRI scanner. The animal auditory stimuli were meticulously edited to a standardised duration of five seconds and subsequently looped to ensure uniformity across the presentation. The sound levels were tested during a pilot study to ensure clarity and comfort for participants. Calibrating the sound intensity to specific

dB levels was avoided to maintain ecological validity and minimise potential distortions in neural responses when comparing diverse vocalisations (e.g., lion's roar vs. cat's meow).

Table 1. The list of stimuli and animal vocalisations.

Trial no.	Animal	Vocalization		
1	Crickets	Chirping		
2	Bear	Growling		
3	Mouse	Squeaking		
4	Tiger	Roaring		
5	Rooster	Crowing		
6	Owl	Hooting		
7	Snake	Hissing		
8	Flies	Buzzing		
9	Wolf	Howling		
10	Cow	Mooing		
11	Sheep	Baaing		
12	Duck	Quacking		
13	Donkey	Braying		
14	Monkey	Chattering		
15	Dog	Barking		
16	Lion	Roaring		
17	Cat	Meowing		
18	Bee	Buzzing		
19	Turkey	Gobbling		
20	Goat	Bleating		
21	Canary Bird	Singing		
22	Crocodile	Bellowing		
23	Goose	Honking		
24	Dolphin	Whistling		
25	Camel	Grunting		
26	Mosquito	Humming		
27	Elephant	Trumpeting		
28	Frog	Croaking		
29	Pig	Oinking		
30	Horse	Neighing		
31	Hen	Clucking		
32	Crow	Cawing		
33	Pigeon	Cooing		
34	Cicada	Buzzing		
35	Parrot	Squawking		

^{*}The corresponding image and audio files are available upon request.

2.3 Data collection methods

Data were collected through questionnaires and fMRI neuroimaging measurements. Demographic information, including age and gender, was obtained through online questionnaires. During the fMRI sessions, blood-oxygen-level-dependent (BOLD) signals and vividness ratings were collected during the imagery tasks.

2.4 Questionnaire

VVIQ was used to assess participants' ability to generate vivid mental images (Marks, 1973). The VVIQ has demonstrated robust reliability and validity in prior research (Cronbach's coefficient α = 0.91, correlation with Gordon test: r = -0.24) (Campos & Pérez-Fabello, 2009; McKelvie, 1995) and widely utilised in studies investigating mental imagery (Dijkstra et al., 2017a; Milton et al., 2021; Tabi et al., 2022). The questionnaire comprises 16 items, each requiring participants to rate the vividness of their mental visualisation of a familiar person, object, or scene on a 5-point scale (1 = no image at all, 5 = perfectly clear and vivid image).

The total score ranges from 16 to 80, with scores below 32 indicatives of poor mental imagery ability, and participants with such scores were not eligible to participate in this study (Zeman et al., 2015). In the present study, the VVIQ scale was adapted to a 0-4 range, aligned with the button-press response options used during fMRI scanning. Consequently, the threshold for normal mental imagery ability was adjusted to a VVIQ score of 16 during participant screening.

2.5 Experimental procedure and design

The evening prior to the fMRI scanning session, participants were provided with the 35 experimental stimuli for review. These stimuli included images and corresponding sounds. Subsequently, they completed an online recognition test, which required them to identify the previously presented image from a set of four options. Researchers developed the online recognition test to assess familiarity with the stimuli. The assessment was administered via Google Forms, with participants instructed to refrain from using study materials during the test. Each section of the test had a 2-minute time limit, and responses were manually reviewed. Participants who achieved a score of 80% or higher were considered familiar with the stimuli and were eligible to participate in the fMRI session the following day. This familiarisation procedure ensured that participants possessed adequate knowledge of the stimuli prior to scanning (Ganis et al., 2004; Lee et al., 2011; Reddy et al., 2010).

Furthermore, participants underwent a practice session outside the scanner, involving five trials of the experimental tasks using non-living object stimuli and their associated (congruent) sounds. This practice session aimed to familiarise participants with the task procedures and minimise potential learning effects during the actual fMRI scan.

To eliminate the potential confounding effects of scanner noise on auditory processing, a sparse temporal sampling (STS) paradigm was employed. This technique involves presenting auditory stimuli during the silent intervals between image acquisitions, thereby reducing the contamination of the BOLD signals by scanner noise (Perrachione & Ghosh, 2013). The STS paradigm ensures that the hemodynamic response captured by fMRI reflects neural activity associated with the auditory stimuli rather than scanner noise

2.6 fMRI paradigm

The fMRI experiment was designed with two distinct phases: the perception phase and the imagery phase. The experimental paradigm is illustrated in **Figure 1**.

In the perception phase, participants were exposed to audiovisual stimuli. They were shown 105 animal images (35 images, each repeated three times in random order) for 5 seconds each, preceded by a 2-second fixation cross. Simultaneously, participants heard the corresponding (congruent) animal sounds through headphones. This phase consisted of 3 runs, each with 18 trials, resulting in a total of 54 trials. A 7-second rest period was provided between each trial, and each run lasted approximately 4 minutes. Participants were also given a 2-minute rest period inside the MRI scanner to allow for relaxation.

The mental imagery phase involved three distinct tasks: image generation, image inspection and vividness

rating. The first task, image generation, required participants to mentally visualise the 35 previously seen animal images upon hearing the corresponding animal sound. The second task, image inspection, involved presenting a pre-recorded statement describing a visual feature of the imagined animal (e.g., "The dog is white"), prompting participants to inspect their mental image for that specific detail.

Lastly, the vividness rating task required participants to evaluate the vividness of their generated mental image on a 1-5 scale (1 = low vividness, 5 = high vividness) adapted from the VVIQ. Because there were only 4 keys on the response device, to avoid confusion, the participants were instructed to rate from 1-4 (key 1, 2, 3 and 4) for scores 2-5, and not to press any key (scoring 0) when there was no image in their mind (scoring 1 in the VVIQ rating scale). The scores obtained were recalculated by adding 1 to each trial for further analysis.

During the imagery phase, participants were instructed to close their eyes and wear an eye mask to minimise external visual distraction (<u>Ganis et al., 2004</u>). The mental imagery phase consisted of 5 runs, each with 11 trials, for a total of 55 trials. Each run lasted approximately 5 minutes, and participants had a 2-minute rest period between runs.

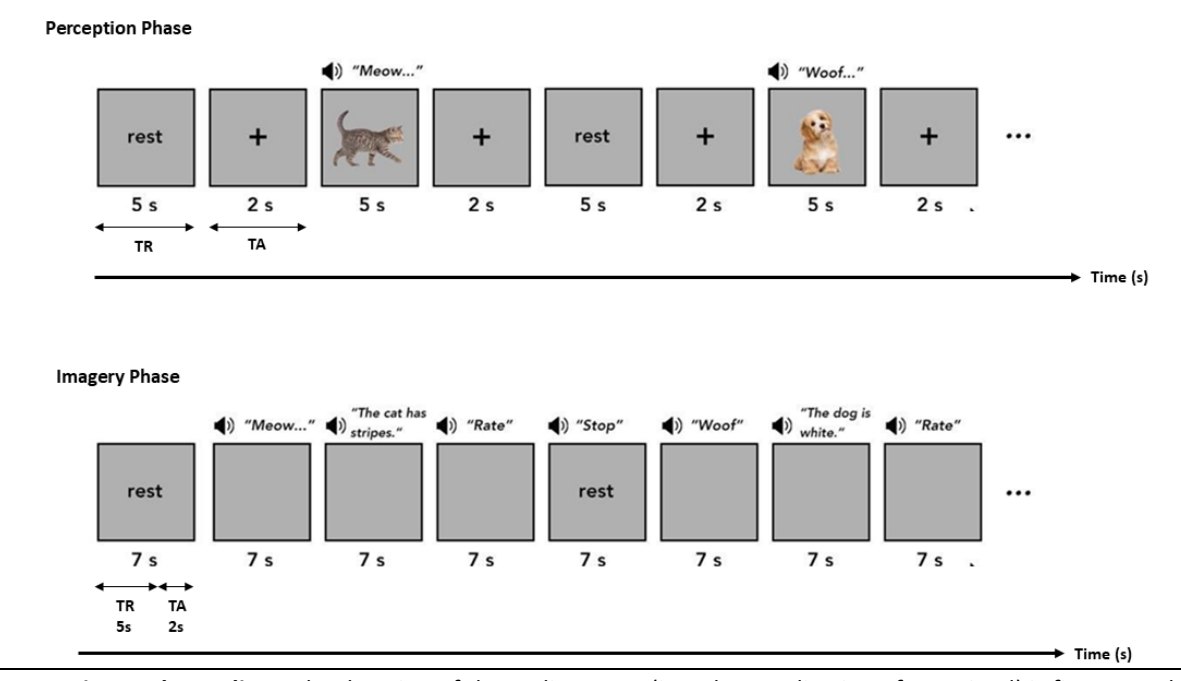


Figure 1. Experimental paradigm. The duration of the auditory cue (i.e., the vocalisation of an animal) is five seconds in both the perception and imagery phases.

2.7 fMRI data acquisition

Both structural and functional images were acquired using a 3T Philips Achieva MRI scanner equipped with 32-channel head coils. High-resolution anatomical images were obtained using a T1-weighted spoiled gradient echo sequence with the following parameters: repetition time (TR) = 1900 msec, echo time (TE) = 2.35 msec, flip angle = 9° , voxel size = $1 \times 1 \times 1$ mm, and matrix size = 256×256 . Functional images sensitive to BOLD contrast were acquired using a T2*-weighted echo planar imaging (EPI) sequence with the following parameters: TR = 7000 msec, TE = 30 msec, TA = 2000 msec, flip angle = 90°, voxel size = 1.5×1.5×3 mm, matrix size = 64×64, sequence = interleaved. T2*-weighted EPI sequences were identical for both perception and imagery phases to ensure consistency in data acquisition across experimental conditions. A 5-second delay was implemented to accommodate the sparse temporal sampling paradigm used in the study (Othman et al., 2020; Perrachione & Ghosh, 2013).

During the functional scans, the perception phase comprised 35 volumes per run, while the imagery phase included 45 volumes per run. The total duration of the scanning session was approximately 65 minutes, comprising 5 minutes for structural scans and 60 minutes for functional scans. Functional scans were organised into multiple runs for both the perception and imagery phases, with 2-minute rest intervals between runs to alleviate participant fatigue. Foam padding was employed to optimise the stabilisation of the head, and participants were provided with explicit instructions to maintain minimal movement throughout the scanning process.

2.8 Data analysis

The acquired fMRI data underwent preprocessing and statistical analysis using Statistical Parametric Mapping (SPM12) software (Functional Imaging Laboratory, Wellcome Department of Imaging Neuroscience, Institute of Neurology, University College of London, UK). Preprocessing steps included slice timing correction, motion correction (realignment), normalisation to the Montreal Neurological Institute (MNI) template, and spatial smoothing using an 8 mm full-width at half-maximum Gaussian kernel (Othman et al., 2020).

For slice-timing correction, the middle slice was used as the reference to minimise temporal discrepancies. The first volume of each run was discarded to mitigate magnetic saturation effects (Othman et al., 2020), and this procedure was consistently applied across both the

perception and imagery phases. After preprocessing, volumes with translational motion exceeding 2 mm or rotational motion exceeding 2° were excluded. A total of 350 functional volumes were included in the final analysis, comprising 34 volumes per run for the perception phase and 44 volumes per run for the imagery phase across multiple runs.

Brain activation patterns, as reflected in BOLD signal changes, were compared between the perception and imagery phases, and across the three imagery tasks (image generation, image inspection, and vividness rating) using random-effects (RFX) analyses with paired t-test and repeated measures ANOVA, respectively. Family-wise error correction (FWE) was applied to control for multiple comparisons, with a significance threshold set at p < 0.05. To enhance sensitivity in cases where voxel-level thresholding did not yield significant results, cluster-level thresholding was utilised (Woo et al., 2014).

Demographic data and vividness rating were analysed using SPSS version 29 (IBM SPSS, Armonk, NY). Pearson Correlation analysis was performed to identify the correlation between the VVIQ scores and vividness rating obtained during the fMRI imagery task. Statistical significance was set at p < 0.05. Numerical data were presented as mean and standard deviation (SD) or median and interquartile range (IQR), depending on the normality of their distribution, as assessed by the Shapiro-Wilk test. Categorical data were presented as frequencies and percentages

3.0 RESULTS

3.1 Demographic data of participants

The demographic information of the participants is presented in **Table 2**. Seven participants (2 males, and 5 females) with a mean age of 22.57 years (SD = 0.48) participated in the study. All participants were right-handed, possessed normal or corrected-to-normal vision, reported normal hearing ability, and denied a history of neurological or psychological diseases. All subjects provided written informed consent for the study.

All participants received the study materials for familiarisation the evening before the scanning and scored over 80 (M=90, SD=2.67) on the recognition test of the images and their related animal sounds, suggesting that they were all familiar with the stimuli. All participants completed the VVIQ (Marks, 1973) with the researcher's instruction and scored above 32,

suggesting that their imagery abilities were within the normal range (M = 66.71, SD = 11.07)

Table 2. Demographic characteristics of participants (n = 7).

Variable	Mean (<i>SD</i>) or Frequency (%)	
Age (yea	22.57 (0.48)	
Gender	Male	2 (28.57)
Gender	Female	5 (71.43)
	Chinese	7 (100.0)
Race	Malay	0 (0)
	Indian	0 (0)
Familiarisatio	90 (2.67)	
VVIQ Sco	66.71 (11.07)	

VVIQ = Vividness of Visual Imagery Questionnaire ; SD = standard deviation.

3.2 Brain activation during perception and imagery

The primary objective of this study was to compare brain activation patterns between visual perception and mental imagery. To directly contrast these conditions, RFX analysis was performed using paired t-tests. At a standard threshold of p < 0.05 (FWE-corrected), no significant differences were observed. However, at a more lenient threshold of p < 0.001 (uncorrected) with cluster-level FWE correction (p < 0.05), perception exhibited significantly higher activation in the right medial superior frontal gyrus (mSFG) compared to imagery (**Table 3 and Figure 2**). In comparison, imagery showed significantly higher activation in the left supplementary motor area (SMA) and right opercular part of the inferior frontal gyrus (OpIFG) (**Table 3 and Figure 2**).

3.3 Brain activation during different imagery tasks

The second research objective was to compare brain activation patterns across the three mental imagery tasks: the image generation task (IG), the image inspection task (II), and the vividness rating task (VR).

The main effect of the task during imagery, assessed using RFX repeated measures ANOVA at p < 0.001 (uncorrected) with cluster-level FWE correction (p < 0.05), revealed a widespread activation across all three imagery tasks (**Table 4 and Figure 3**). The most prominent activation was observed in the left superior parietal lobule (SPL) and right SMA, followed by the left OpIFG, left superior temporal gyrus (STG) and right cerebellum VI.

Contrasting IG with the II showed heightened activation during IG in regions associated with auditory processing

and language comprehension, including the bilateral left STG (**Table 4 and Figure 4**). No regions showed significantly higher activation for II compared to IG.

Comparing IG to VR revealed greater activation during IG (**Table 4 and Figure 4**) in the left SPL, left STG, left triangular part of the inferior frontal gyrus (triIFG), right SMA, and left precuneus suggesting a broader network for IG involving attentional control, auditory and linguistic processing, semantic processing, motor planning, and self-referential processing and memory retrieval. A comparison between II and VR revealed no brain regions with significantly higher activation.

Contrasting II with VR showed higher activation during II in the left thalamus, left middle frontal gyrus (MFG), right cerebellum VI, right SMA, and left postcentral gyrus, indicating greater demands on attention, decision-making, and sensory integration during image inspection compared to vividness rating.

Overall, the imagery phase highlights the dynamic engagement of a distributed brain network encompassing regions associated with visual processing, auditory processing, motor planning, and cognitive control. The specific pattern of activation varied across the three imagery tasks, suggesting that distinct cognitive processes are recruited during the generation, inspection, and evaluation of mental images

3.4 Behavioural results: VVIQ and vividness ratings

The relationship between participants' pre-scan VVIQ scores and their in-scanner vividness rating during the imagery task was examined (**Tables 5 and 6**). The VVIQ scores and the vividness ratings were both normally distributed, as confirmed by the Shapiro-Wilk test (**Table 4**). Pearson correlation analysis revealed a strong positive correlation between these two measures (r = 0.79, p = 0.033). This indicates that participants who reported higher baseline imagery vividness on the VVIQ also tended to provide higher vividness ratings for their mental images during the fMRI task.

4.0 DISCUSSION

The present findings contribute to the ongoing discourse on the neural overlap and divergence between perception and imagery. The results confirm the existence of substantial shared neural substrates, while also highlighting subtle yet significant differences in activation patterns, particularly in higher-order cortical regions associated with attentional control, motor planning and inhibition. The heightened activation of the right mSFG during perception aligns

Table 3. Brain activation differences between visual perception and mental imagery: paired t-test random-effects (RFX) results at p < 0.001 (uncorrected) with cluster-level family-wise error (FWE) corrected (p < 0.05).

Combined	Region Label	Extent	t-value	Effect Size	MNI Coordinates		
Contrast	(BA)	(No. of voxels)		(Hedges' g)	х	у	Z
Perception > Imagery	Right mSFG (BA10)	51	16.51	7.68	6	56	14
Imagery > Perception	Left SMA (BA6)	96	13.11	6.11	-3	5	59
	Right OpIFG (BA45)	56	12.38	5.77	47	20	14

BA = Brodmann Area; MNI = Montreal Neurological Institute template; mSFG = medial superior frontal gyrus; OpIFG = opercular part of inferior frontal gyrus; SMA = supplementary motor area.

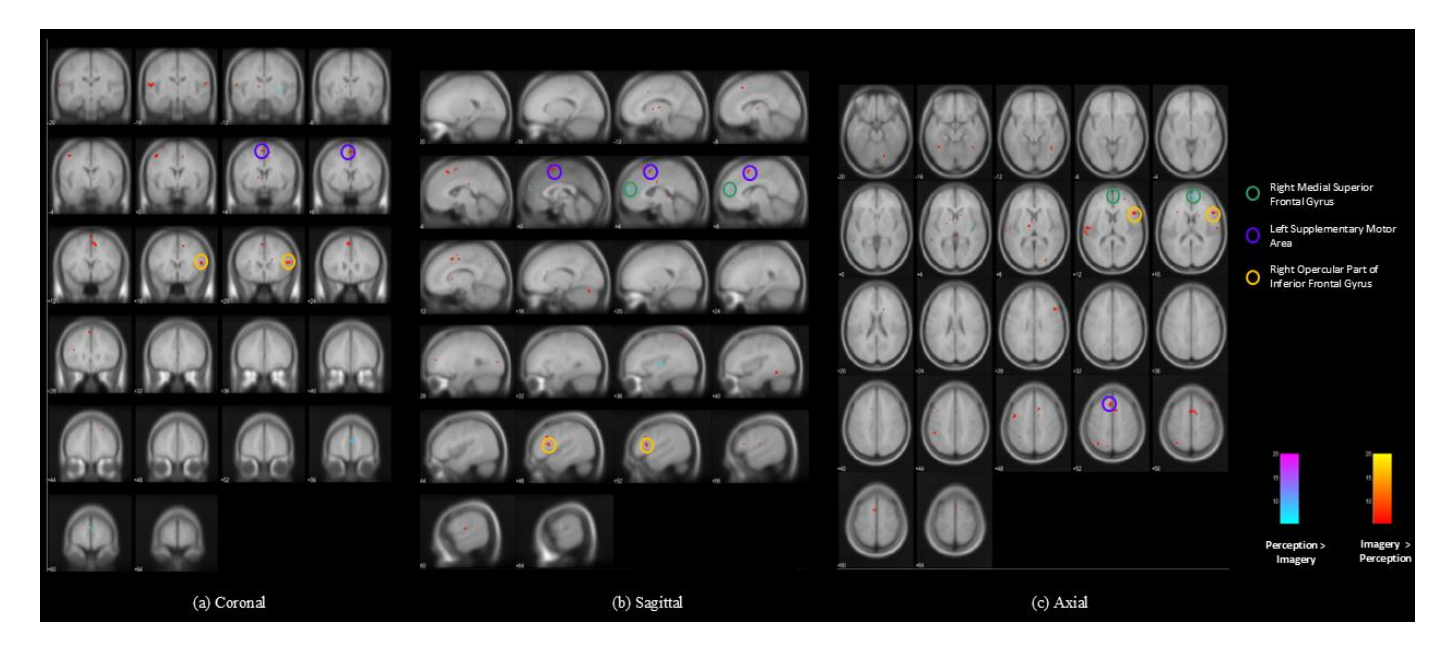


Figure 2. Brain activation differences between visual perception and mental imagery, paired t-test RFX results (p < 0.001, uncorrected with cluster-level FWE corrected, p < 0.05). (a) Coronal, (b) sagittal, and (c) axial views. Green circles indicate activation in the right mSFG, purple circles indicate activation in the left SMA, and orange circles indicate activation in the right OpIFG.

Table 4. Brain activation across three mental imagery tasks (IG, II and VR) at p < 0.001 (uncorrected) with cluster-level FWE correction (p < 0.05).

Contrast	Region Label	Extent	. A volue	Effect Size	MM	MNI Coordinates		
Contrast	(BA)	(No. of voxels)	t-value	(Hedges' g)	х	у	Z	
	Left SPL (BA7)	84	40.95	19.08	-30	-66	56	
	Right SMA (BA6)	107	26.22	12.22	2	7	56	
Main effect	Left OpIFG (NA)	96	25.68	12.00	-45	16	32	
	Left STG (BA42)	66	25.62	11.94	-59	-13	11	
	Right cerebellum VI (NA)	63	24.73	11.52	15	-60	-19	
	Left STG (BA42)	266	7.75	3.61	-64	-25	11	
10 > 11	Right STG (NA)	101	7.27	3.39	65	-25	14	
IG > II	Left STG (BA13)	134	7.00	3.26	-46	-36	20	
	Right STG (NA)	193	6.68	3.11	57	-3	2	
	Left SPL (BA7)	160	9.05	4.21	-30	-66	56	
IG > VR	Left STG (BA42)	166	8.96	4.17	-64	-25	11	
	Left triIFG (NA)	247	6.99	3.26	-44	18	29	
	Right SMA (BA6)	228	6.99	3.26	2	6	56	
	Left Precuneus (NA)	85	6.15	2.86	-4	-74	38	

Continued on next page

	Left Thalamus (NA)	121	11.62	5.41	-16	-22	14
II S VD	Left MFG (NA)	141	8.07	3.76	-32	43	32
II > VR	Right cerebellum VI (NA)	298	7.03	3.28	15	-60	-19
	Right SMA (NA)	178	6.25	2.92	2	-1	59

BA = Brodmann Area; IG = Image Generation; II = Image Inspection; MFG = middle frontal gyrus; MNI = Montreal Neurological; NA = not available; Institute template; OpIFG = opercular part of inferior frontal gyrus; SMA = supplementary motor area; SPL = superior parietal lobule; STG = superior temporal gyrus, triIFG = triangular part of left inferior frontal gyrus; VR = Vividness Rating.

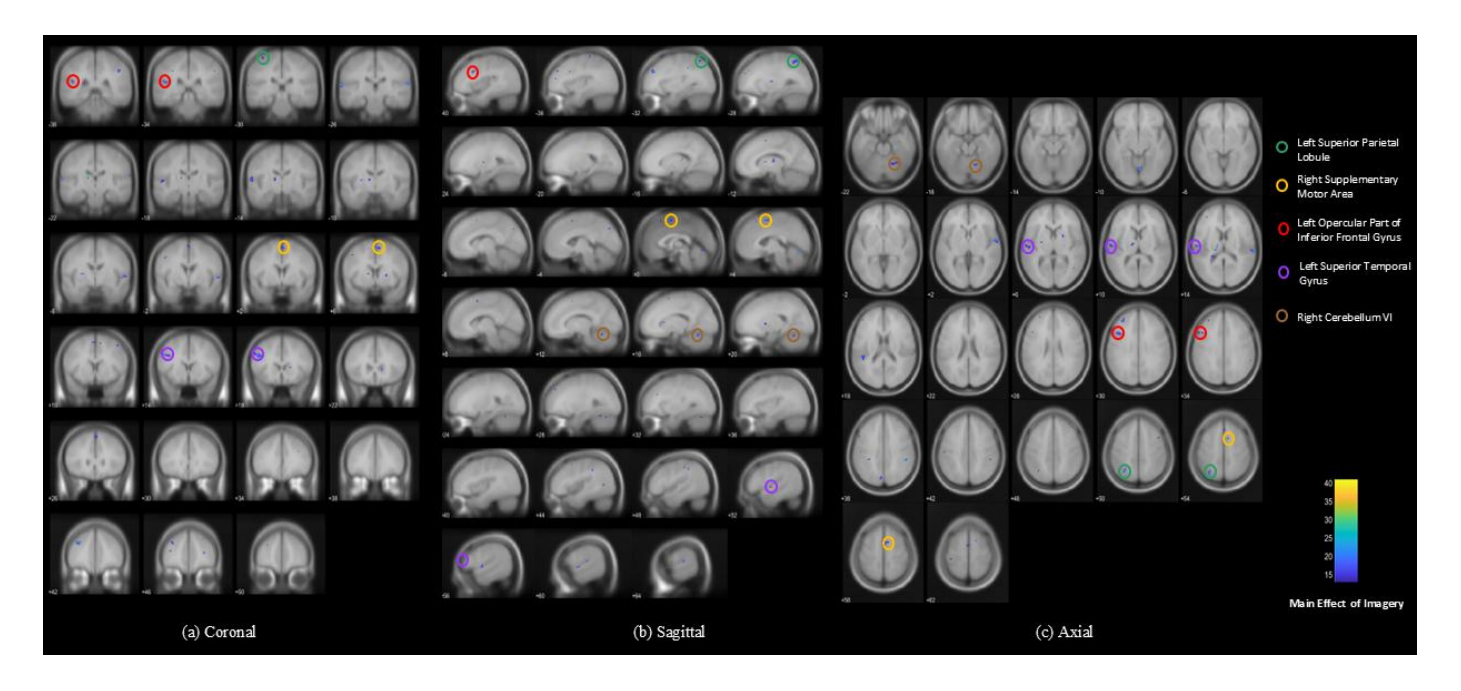


Figure 3. Brain activation for the main effect of imagery (p < 0.001, uncorrected with cluster-level FWE corrected p < 0.05). (a) Coronal, (b) sagittal, and (c) axial views. Green circles indicate activation in the left SPL, orange circles indicate activation in the right SMA, red circles indicate activation in the left OpIFG, purple circles indicate activation in the left STG, and brown circles indicate activation in the right cerebellum VI.

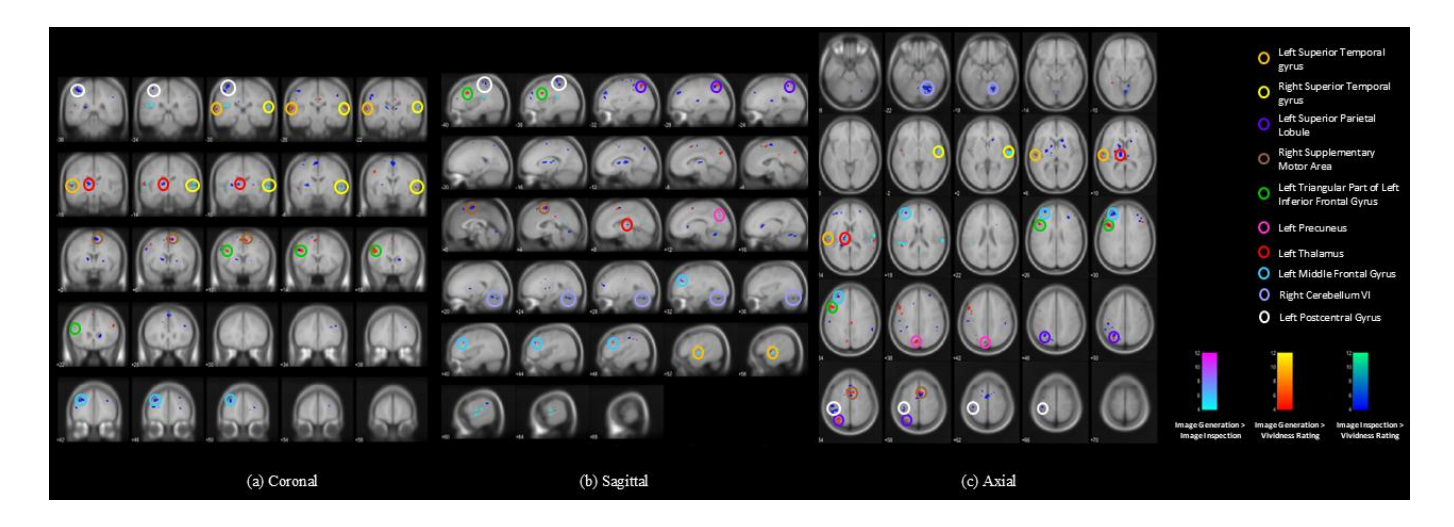


Figure 4. Brain activation differences between the mental imagery task (p < 0.001, uncorrected with cluster-level FWE corrected p < 0.05). (a) Coronal, (b) sagittal, and (c) axial views. Orange and yellow circles indicate activation in the left and right STG respectively, purple circles indicate activation in the left SPL, brown circles indicate right SMA, green circles indicate activation in the left precuneus, red circles indicate activation in the left thalamus, light blue circles indicate activation in the left MFG, purple circles indicate activation in the right cerebellum VI and white circles indicate activation in the left postcentral gyrus.

with its role in top-down attentional control and the integration of sensory information (<u>Corbetta & Shulman, 2002</u>). The mSFG's involvement in guiding attentional focus and selecting relevant sensory input likely contributes to the active processing of external stimuli during perception.

In contrast, the increased activation of the left SMA and right OpIFG during imagery suggests a greater reliance on internal representation and cognitive control. The SMA's well-established role in motor planning and the OpIFG's involvement in response inhibition and attentional control highlight the active nature of imagery, requiring the construction and maintenance of mental representations in the absence of external sensory input (Aron et al., 2004; Nachev et al., 2008). The heightened OpIFG activation during imagery may also reflect the need to suppress irrelevant information and maintain focus on the imagined content (Hampshire et al., 2010).

Table 5. Normality tests for VVIQ and vividness rating score.

Variable	Shapiro-Wilk test					
	W	df	p-value			
VVIQ	0.94	7	0.62			
VR	0.97	7	0.91			

Table 6. Correlation between VVIQ scores and in-scanner vividness ratings.

Variable	VVIQ	VR	p-value	R
Score	66.71	199.00	0.033	0.79
	(11.07)	(22.81)		

VVIQ = Vividness of Visual Imagery Questionnaire ; VR = vividness rating task.

The analysis of the main effect of the task during the imagery phase revealed a widespread network of brain regions, underscoring the complexity of mental imagery and the dynamic interplay of various brain regions. The prominent activation observed in the left SPL and right SMA aligns with their roles within the frontoparietal network, a system crucial for cognitive control and attention (Cole & Schneider, 2007). The SPL's involvement in spatial attention and the SMA's contribution to motor planning suggest the importance of these processes in mentally manipulating and interacting with imagined objects (Koenigs et al., 2009). The activation of the OpIFG and STG further emphasises the role of the frontoparietal network in integrating sensory information and language processing, particularly when auditory cues trigger imagery (<u>Binder</u> et al., 1997).

Moreover, the involvement of cerebellum VI suggests its contribution to the coordination and fine-tuning of mental imagery processes, consistent with its role in various cognitive functions beyond motor control (Koziol et al., 2014). The primary effect of task analysis highlights the distributed nature of the neural network underlying mental imagery, underscoring the diverse cognitive processes involved in generating, inspecting, and evaluating mental images.

The distinct activation patterns observed across the three mental imagery tasks (IG, II and VR) further illuminate the involvement of both shared and unique neural substrates in different aspects of mental imagery. The IG task, which requires the construction of mental images based on auditory cues, elicited greater activation in regions associated with auditory processing and language comprehension, suggesting an increased reliance on auditory and linguistic representations during the initial formation of mental images (Hubbard, 2010).

Furthermore, the heightened activation in the left SPL, left trilFG, right SMA, and left precuneus during IG underscores the recruitment of a broader neural network for attentional control, semantic processing, motor planning, and self-referential processing, reflecting the complex cognitive demands of this task (Cabeza & Nyberg, 2000; Cavanna & Trimble, 2006; Corbetta & Shulman, 2002; Nachev et al., 2008). The distinct pattern of brain activation observed during IG, compared to VR, suggests that generating a mental image involves a more extensive network of brain regions responsible for attentional control, auditory and linguistic processing, semantic processing, motor planning, and self-referential processing.

Interestingly, no brain regions exhibited significantly higher activation during the VR task compared to the IG or II conditions. Similarly, no brain regions were more active during the II condition compared to the IG condition. This suggests that while IG engages a broader network, II and VR do not necessarily recruit additional unique regions beyond those involved in IG. This suggests that the neural processes underlying the subjective evaluation of mental image vividness might share considerable overlap with those involved in generating and inspecting mental images. This observation aligns with previous research suggesting a close relationship between the ability to generate vivid

mental images and the subjective experience of vividness (Dijkstra et al., 2017b).

The heightened activation in the left thalamus and left MFG during II compared to VR suggests that maintaining and inspecting a mental image may necessitate greater attentional focus, decision-making, and sensory integration (Asanowicz et al., 2021; Klein-Flügge et al., 2022; Laakso et al., 2019; McCormick & Bal, 1994; Van Noordt et al., 2022). The MFG acts as a central executive, performing task-relevant operations (Bugatus et al., 2017). These findings align with previous studies reporting inhibitory effects within the frontal network during visual creative imagery (Cai et al., 2018; Pidgeon et al., 2016). This suggests that maintaining and inspecting a mental image may necessitate greater attentional focus and decision-making compared to simply evaluating its vividness.

The distinct activation patterns observed across the three mental imagery tasks highlight the involvement of both shared and unique neural substrates in different aspects of mental imagery. The IG task, relying heavily on auditory and linguistic processing, engages a broader network of brain regions compared to image inspection and vividness rating. The latter two tasks, while sharing neural substrates with IG, also recruit distinct regions associated with cognitive control, decision-making, and sensory integration. These findings highlight the dynamic and flexible nature of the neural network underlying mental imagery, which adapts to the specific demands of each task.

The behavioural results of this study further support the intricate relationship between the subjective experience of visual imagery and its neural underpinnings. The strong positive correlation observed between participants' pre-scan VVIQ scores and their inscanner VR during the imagery task (r = 0.79, p = 0.033) suggests that individuals who report higher baseline imagery vividness on the VVIQ also tend to experience more vivid mental images during fMRI tasks. This finding aligns with previous research demonstrating a close association between self-reported imagery vividness objective measures ability of imagery (Dijkstra et al., 2017b; Pearson et al., 2011).

The consistency between subjective ratings and neural activation patterns during imagery tasks highlights the validity of self-report measures in capturing individual differences in imagery vividness. Furthermore, it suggests that the VR task employed in this study effectively elicited brain activity related to the

subjective experience of visual imagery. The robust correlation between VVIQ scores and in-scanner vividness ratings underscores the potential of this paradigm for future investigations into the neural correlates of the vividness of visual imagery and its role in various cognitive functions

While this study provides valuable insights into the neural underpinnings of perception and imagery, several limitations need to be acknowledged. First, although the use of RFX analysis mitigates some concerns related to the small sample size (N = 7), the observed effect sizes were generally large, suggesting the potential for replication even with a larger sample. However, further research with a larger cohort is necessary to validate and generalise the current findings. Second, despite the implementation of the STS technique, the presence of scanner noise during auditory stimulus presentation could potentially impact the observed activation patterns.

Future studies could explore alternative neuroimaging modalities, such as electroencephalography (EEG) or magnetoencephalography (MEG), to overcome this limitation. Finally, while the study incorporated VR as a subjective measure of imagery experience, future research could benefit from including additional behavioural measures, such as reaction times or accuracy in image recognition tasks, to gain a more comprehensive understanding of the behavioural correlates of brain activation during perception and imagery.

These findings highlight the complex and multifaceted nature of mental imagery, providing further evidence for the distinct neural processes underlying different aspects of this cognitive phenomenon.

5.0 CONCLUSION

In conclusion, this study offers novel insights into the neural mechanisms underlying perception and imagery, utilising a combination of fMRI and STS paradigms. Our findings underscore the complex interplay between these two cognitive processes, highlighting both shared and distinct neural substrates. The results also emphasise the dynamic nature of mental imagery and the diverse cognitive processes involved in its different stages. The distinct activation patterns observed during IG, II, and VR suggest that targeted interventions could be developed to enhance specific aspects of mental imagery, which could have implications for improving cognitive functions such as memory, creativity, and problem-solving. Future research with larger sample

sizes and additional behavioural measures could further elucidate the intricate relationship between perception and imagery, paving the way for a more comprehensive understanding of the human mind and its remarkable capacity for mental representation

Acknowledgements:

The authors declare that this research project is funded by the Bench Fee of Cognitive Neurosciences Programme (401/PPSP/E3170003). We extend our sincere appreciation to Encik Hazim Omar for his valuable knowledge and assistance in data collection and the development of the task paradigm. We also gratefully acknowledge the significant contributions

of Puan Wan Nazyrah, Puan Afidah, and Puan Che Munirah, the radiographers at the Radiology Department, Hospital Universiti Sains Malaysia.

Author Contributions:

GY & AIAH administered the project, designed the fMRI paradigm, and analysed the data; GY performed the experiment and wrote the initial draft of the manuscript; HU conceptualised the initial idea; AIAH & HU planned the experimental procedure, reviewed and edited the manuscript.

Conflicts of Interest:

The authors declared no conflict of interest.

REFERENCES

- Albers, A. M., Kok, P., Toni, I., Dijkerman, H. C., & De Lange, F. P. (2013). Shared representations for working memory and mental imagery in early visual cortex. *Current Biology*, 23(15), 1427–1431. https://doi.org/10.1016/j.cub.2013.05.065
- Amedi, A., Malach, R., & Pascual-Leone, A. (2005). Negative BOLD differentiates visual imagery and perception. *Neuron*, 48(5), 859–872. https://doi.org/10.1016/j.neuron.2005.10.032
- Aron, A. R., Robbins, T. W., & Poldrack, R. A. (2004). Inhibition and the right inferior frontal cortex. *Trends in Cognitive Sciences*, 8(4), 170–177. https://doi.org/10.1016/j.tics.2004.02.010
- Asanowicz, D., Panek, B., & Kotlewska, I. (2021). Selection for action: The medial frontal cortex is an executive hub for stimulus and response selection. *Journal of Cognitive Neuroscience*, *33*(8), 1442–1469. https://doi.org/10.1162/jocn_a_01727
- Bartolomeo, P., Bachoud-Lévi, A., De Gelder, B., Denes, G., Barba, G. D., Brugières, P., & Degos, J. (1998). Multiple-domain dissociation between impaired visual perception and preserved mental imagery in a patient with bilateral extrastriate lesions. *Neuropsychologia*, *36*(3), 239–249. https://doi.org/10.1016/s0028-3932(97)00103-6
- Bartolomeo, P., Bachoud-Lévi, A., & De Schotten, M. T. (2013). The anatomy of cerebral achromatopsia: A reappraisal and comparison of two case reports. *Cortex*, *56*, 138–144. https://doi.org/10.1016/j.cortex.2013.01.013
- Binder, J. R., Frost, J. A., Hammeke, T. A., Cox, R. W., Rao, S. M., & Prieto, T. (1997). Human brain language areas identified by functional magnetic resonance imaging. *Journal of Neuroscience*, *17*(1), 353–362. https://doi.org/10.1523/jneurosci.17-01-00353.1997
- Boccia, M., Sulpizio, V., Bencivenga, F., Guariglia, C., & Galati, G. (2021). Neural representations underlying mental imagery as unveiled by representation similarity analysis. *Brain Structure and Function*, 226(5), 1511–1531. https://doi.org/10.1007/s00429-021-02266-z
- Breedlove, J. L., St-Yves, G., Olman, C. A., & Naselaris, T. (2020). Generative feedback explains distinct brain activity codes for seen and mental images. *Current Biology*, *30*(12), 2211-2224.e6. https://doi.org/10.1016/j.cub.2020.04.014
- Bugatus, L., Weiner, K. S., & Grill-Spector, K. (2017). Task alters category representations in prefrontal but not high-level visual cortex. *NeuroImage*, *155*, 437–449. https://doi.org/10.1016/j.neuroimage.2017.03.062
- Cabeza, R., & Nyberg, L. (2000). Imaging cognition II: an empirical review of 275 PET and FMRI studies. *Journal of Cognitive Neuroscience*, 12(1), 1–47. https://doi.org/10.1162/08989290051137585
- Cai, Y., Zhang, D., Liang, B., Wang, Z., Li, J., Gao, Z., Gao, M., Chang, S., Jiao, B., Huang, R., & Liu, M. (2018). Relation of visual creative imagery manipulation to resting-state brain oscillations. *Brain Imaging and Behavior*, *12*(1), 258–273. https://doi.org/10.1007/s11682-017-9689-8
- Campos, A., & Pérez-Fabello, M. J. (2009). Psychometric quality of a revised version vividness of visual imagery questionnaire. *Perceptual and Motor Skills*, 108(3), 798–802. https://doi.org/10.2466/pms.108.3.798-802
- Cavanna, A. E., & Trimble, M. R. (2006). The precuneus: a review of its functional anatomy and behavioural correlates. *Brain*, 129(3), 564–583. https://doi.org/10.1093/brain/awl004
- Cole, M. W., & Schneider, W. (2007). The cognitive control network: integrated cortical regions with dissociable functions. *NeuroImage*, *37*(1), 343–360. https://doi.org/10.1016/j.neuroimage.2007.03.071
- Corbetta, M., & Shulman, G. L. (2002). Control of goal-directed and stimulus-driven attention in the brain. *Nature Reviews. Neuroscience*, *3*(3), 201–215. https://doi.org/10.1038/nrn755
- De Borst, A. W., Sack, A. T., Jansma, B. M., Esposito, F., De Martino, F., Valente, G., Roebroeck, A., Di Salle, F., Goebel, R., & Formisano, E. (2011). Integration of "what" and "where" in frontal cortex during visual imagery of scenes. *NeuroImage*, 60(1), 47–58. https://doi.org/10.1016/j.neuroimage.2011.12.005

- De Gelder, B., Tamietto, M., Pegna, A. J., & Van Den Stock, J. (2014). Visual imagery influences brain responses to visual stimulation in bilateral cortical blindness. *Cortex*, 72, 15–26. https://doi.org/10.1016/j.cortex.2014.11.009
- Dijkstra, N., Bosch, S. E., & Van Gerven, M. A. (2017a). Vividness of visual imagery depends on the neural overlap with perception in visual areas. *Journal of Neuroscience*, *37*(5), 1367–1373. https://doi.org/10.1523/jneurosci.3022-16.2016
- Dijkstra, N., Bosch, S. E., & Van Gerven, M. A. (2019). Shared neural mechanisms of visual perception and imagery. *Trends in Cognitive Sciences*, 23(5), 423–434. https://doi.org/10.1016/j.tics.2019.02.004
- Dijkstra, N., Zeidman, P., Ondobaka, S., Van Gerven, M. a. J., & Friston, K. (2017b). Distinct top-down and bottom-up brain connectivity during visual perception and imagery. *Scientific Reports*, 7(1), 5677. https://doi.org/10.1038/s41598-017-05888-8
- Fulford, J., Milton, F., Salas, D., Smith, A., Simler, A., Winlove, C., & Zeman, A. (2017). The neural correlates of visual imagery vividness An fMRI study and literature review. *Cortex*, *105*, 26–40. https://doi.org/10.1016/j.cortex.2017.09.014
- Ganis, G. (2013). *Visual mental imagery*. Multisensory Imagery (pp. 9–28). Springer Publishing, United States. https://doi.org/10.1007/978-1-4614-5879-1 2
- Ganis, G., Thompson, W. L., & Kosslyn, S. M. (2004). Brain areas underlying visual mental imagery and visual perception: an fMRI study. *Cognitive Brain Research*, 20(2), 226–241. https://doi.org/10.1016/j.cogbrainres.2004.02.012
- Hampshire, A., Chamberlain, S. R., Monti, M. M., Duncan, J., & Owen, A. M. (2010). The role of the right inferior frontal gyrus: inhibition and attentional control. *NeuroImage*, *50*(3), 1313–1319. https://doi.org/10.1016/j.neuroimage.2009.12.109
- Hubbard, T. L. (2010). Auditory imagery: Empirical findings. *Psychological Bulletin*, *136*(2), 302–329. https://doi.org/10.1037/a0018436
- Johnson, M. R., & Johnson, M. K. (2014). Decoding individual natural scene representations during perception and imagery. Frontiers in Human Neuroscience, 8, 059. https://doi.org/10.3389/fnhum.2014.00059
- Klein-Flügge, M. C., Bongioanni, A., & Rushworth, M. F. (2022). Medial and orbital frontal cortex in decision-making and flexible behavior. *Neuron*, *110*(17), 2743–2770. https://doi.org/10.1016/j.neuron.2022.05.022
- Koenig-Robert, R., & Pearson, J. (2020). Why do imagery and perception look and feel so different? *Philosophical Transactions of the Royal Society B Biological Sciences*, *376*(1817), 20190703. https://doi.org/10.1098/rstb.2019.0703
- Koenigs, M., Barbey, A. K., Postle, B. R., & Grafman, J. (2009). Superior parietal cortex is critical for the manipulation of information in working memory. *Journal of Neuroscience*, *29*(47), 14980–14986. https://doi.org/10.1523/jneurosci.3706-09.2009
- Kosslyn, S. M. (2005). Mental images and the brain. *Cognitive Neuropsychology*, 22(3–4), 333–347. https://doi.org/10.1080/02643290442000130
- Koziol, L. F., Budding, D., Andreasen, N., D'Arrigo, S., Bulgheroni, S., Imamizu, H., Ito, M., Manto, M., Marvel, C., Parker, K., Pezzulo, G., Ramnani, N., Riva, D., Schmahmann, J., Vandervert, L., & Yamazaki, T. (2014). Consensus paper: the cerebellum's role in movement and cognition. *The Cerebellum*, 13(1), 151–177. https://doi.org/10.1007/s12311-013-0511-x
- Laakso, H. M., Hietanen, M., Melkas, S., Sibolt, G., Curtze, S., Virta, M., Ylikoski, R., Pohjasvaara, T., Kaste, M., Erkinjuntti, T., & Jokinen, H. (2019). Executive function subdomains are associated with post-stroke functional outcome and permanent institutionalization. *European Journal of Neurology*, *26*(3), 546–552. https://doi.org/10.1111/ene.13854
- Lee, S., Kravitz, D. J., & Baker, C. I. (2011). Disentangling visual imagery and perception of real-world objects. *NeuroImage*, 59(4), 4064–4073. https://doi.org/10.1016/j.neuroimage.2011.10.055
- Marks, D. F. (1973). Visual imagery differences in the recall of pictures. *British Journal of Psychology*, *64*(1), 17–24. https://doi.org/10.1111/j.2044-8295.1973.tb01322.x
- Marks, D. F. (1995). New directions for Mental Imagery Research. *Journal of Mental Imagery, 19*(3–4), 153–167. https://psycnet.apa.org/record/1996-29150-001
- McCormick, D. A., & Bal, T. (1994). Sensory gating mechanisms of the thalamus. *Current Opinion in Neurobiology*, *4*(4), 550–556. https://doi.org/10.1016/0959-4388(94)90056-6
- McKelvie, S. J. (1995). The VVIQ as a psychometric test of individual differences in visual imagery vividness: A critical quantitative review and plea for direction. *Journal of Mental Imagery, 19*(3–4), 1–106. https://psycnet.apa.org/record/1996-29151-001
- Milton, F., Fulford, J., Dance, C., Gaddum, J., Heuerman-Williamson, B., Jones, K., Knight, K. F., MacKisack, M., Winlove, C., & Zeman, A. (2021). Behavioral and neural signatures of visual imagery vividness extremes: aphantasia versus hyperphantasia. *Cerebral Cortex Communications*, *2*(2), tgab035. https://doi.org/10.1093/texcom/tgab035
- Moro, V., Berlucchi, G., Lerch, J., Tomaiuolo, F., & Aglioti, S. M. (2007). Selective deficit of mental visual imagery with intact primary visual cortex and visual perception. *Cortex*, *44*(2), 109–118. https://doi.org/10.1016/j.cortex.2006.06.004
- Morozova, M., Nasibullina, A., Yakovlev, L., Syrov, N., Kaplan, A., & Lebedev, M. (2024). Tactile versus motor imagery: differences in corticospinal excitability assessed with single-pulse TMS. *Scientific Reports*, *14*(1), 14862. https://doi.org/10.1038/s41598-024-64665-6
- Mountcastle, V. (1997). The columnar organization of the neocortex. *Brain*, 120(4), 701–722. https://doi.org/10.1093/brain/120.4.701

- Nachev, P., Kennard, C., & Husain, M. (2008). Functional role of the supplementary and pre-supplementary motor areas. *Nature Reviews. Neuroscience*, *9*(11), 856–869. https://doi.org/10.1038/nrn2478
- Naselaris, T., Olman, C. A., Stansbury, D. E., Ugurbil, K., & Gallant, J. L. (2015). A voxel-wise encoding model for early visual areas decodes mental images of remembered scenes. *NeuroImage*, *105*, 215–228. https://doi.org/10.1016/j.neuroimage.2014.10.018
- Othman, E. A., Yusoff, A. N., Mohamad, M., Manan, H. A., Hamid, A. I. A., & Giampietro, V. (2020). Hemispheric lateralization of auditory working memory regions during stochastic resonance: an FMRI study. *Journal of Magnetic Resonance Imaging*, *51*(6), 1821–1828. https://doi.org/10.1002/jmri.27016
- Pearson, J., Rademaker, R. L., & Tong, F. (2011). Evaluating the mind's eye. *Psychological Science*, *22*(12), 1535–1542. https://doi.org/10.1177/0956797611417134
- Perrachione, T. K., & Ghosh, S. S. (2013). Optimized design and analysis of Sparse-Sampling FMRI experiments. *Frontiers in Neuroscience*, 7, 055. https://doi.org/10.3389/fnins.2013.00055
- Perry, C. J., & Fallah, M. (2014). Feature integration and object representations along the dorsal stream visual hierarchy. Frontiers in Computational Neuroscience, 8, 084. https://doi.org/10.3389/fncom.2014.00084
- Pidgeon, L. M., Grealy, M., Duffy, A. H. B., Hay, L., McTeague, C., Vuletic, T., Coyle, D., & Gilbert, S. J. (2016). Functional neuroimaging of visual creativity: a systematic review and meta-analysis. *Brain and Behavior*, *6*(10), e00540. https://doi.org/10.1002/brb3.540
- Ragni, F., Lingnau, A., & Turella, L. (2021). Decoding category and familiarity information during visual imagery. *NeuroImage*, 241, 118428. https://doi.org/10.1016/j.neuroimage.2021.118428
- Reddy, L., Tsuchiya, N., & Serre, T. (2010). Reading the mind's eye: Decoding category information during mental imagery. *NeuroImage*, 50(2), 818–825. https://doi.org/10.1016/j.neuroimage.2009.11.084
- Riesenhuber, M., & Poggio, T. (1999). Hierarchical models of object recognition in cortex. *Nature Neuroscience*, *2*(11), 1019–1025. https://doi.org/10.1038/14819
- Slotnick, S. D., Thompson, W. L., & Kosslyn, S. M. (2005). Visual mental imagery induces retinotopically organized activation of early visual areas. *Cerebral Cortex*, *15*(10), 1570–1583. https://doi.org/10.1093/cercor/bhi035
- Spagna, A., Hajhajate, D., Liu, J., & Bartolomeo, P. (2021). Visual mental imagery engages the left fusiform gyrus, but not the early visual cortex: A meta-analysis of neuroimaging evidence. *Neuroscience & Biobehavioral Reviews*, 122, 201–217. https://doi.org/10.1016/j.neubiorev.2020.12.029
- Sulfaro, A. A., Robinson, A. K., & Carlson, T. A. (2023). Modelling perception as a hierarchical competition differentiates imagined, veridical, and hallucinated percepts. *Neuroscience of Consciousness*, 2023(1), niad018. https://doi.org/10.1093/nc/niad018
- Tabi, Y. A., Maio, M. R., Attaallah, B., Dickson, S., Drew, D., Idris, M. I., Kienast, A., Klar, V., Nobis, L., Plant, O., Saleh, Y., Sandhu, T. R., Slavkova, E., Toniolo, S., Zokaei, N., Manohar, S. G., & Husain, M. (2022). Vividness of visual imagery questionnaire scores and their relationship to visual short-term memory performance. *Cortex*, *146*, 186–199. https://doi.org/10.1016/j.cortex.2021.10.011
- Thorudottir, S., Sigurdardottir, H. M., Rice, G. E., Kerry, S. J., Robotham, R. J., Leff, A. P., & Starrfelt, R. (2020). The architect who lost the ability to imagine: the cerebral basis of visual imagery. *Brain Sciences*, *10*(2), 59. https://doi.org/10.3390/brainsci10020059
- Umar, H., Mast, F. W., Cacchione, T., & Martarelli, C. S. (2021). The prioritization of visuo-spatial associations during mental imagery. *Cognitive Processing*, 22(2), 227–237. https://doi.org/10.1007/s10339-020-01010-5
- Van Noordt, S., Heffer, T., & Willoughby, T. (2022). A developmental examination of medial frontal theta dynamics and inhibitory control. *NeuroImage*, *246*, 118765. https://doi.org/10.1016/j.neuroimage.2021.118765
- Winlove, C. I., Milton, F., Ranson, J., Fulford, J., MacKisack, M., Macpherson, F., & Zeman, A. (2018). The neural correlates of visual imagery: A co-ordinate-based meta-analysis. *Cortex*, 105, 4–25. https://doi.org/10.1016/j.cortex.2017.12.014
- Woo, C., Krishnan, A., & Wager, T. D. (2014). Cluster-extent based thresholding in fMRI analyses: Pitfalls and recommendations. *NeuroImage*, *91*, 412–419. https://doi.org/10.1016/j.neuroimage.2013.12.058
- World Health Organization. (2018, March 1). WHO launches the HearWHO app for mobile devices to help detect hearing loss. WHO Newsletters. https://www.who.int/news/item/01-03-2018-who-launches-the-hearwho-app-for-mobile-devices-to-help-detect-hearing-loss
- Xie, S., Kaiser, D., & Cichy, R. M. (2020). Visual imagery and perception share neural representations in the alpha frequency band. *Current Biology*, *30*(13), 2621-2627.e5. https://doi.org/10.1016/j.cub.2020.04.074
- Zeman, A., Dewar, M., & Della Sala, S. (2015). Lives without imagery congenital aphantasia. *Cortex, 73,* 378–380. https://doi.org/10.1016/j.cortex.2015.05.019